Design, Control and Validation of the Variable Stiffness Exoskeleton FLExo

Sariah Mghames[1], Marco Laghi[1,2], Cosimo Della Santina[1], Manolo Garabini[1], Manuel Catalano[2], Giorgio Grioli[2] and Antonio Bicchi[1,2]

***Abstract*— In this paper we present the design of a one degree of freedom assistive platform to augment the strength of upper limbs. The core element is a variable stiffness actuator, closely reproducing the behavior of a pair of antagonistic muscles.**

The novelty introduced by this device is the analogy of its control parameters with those of the human muscle system, the threshold lengths. The analogy can be obtained from a proper tuning of the mechanical system parameters. Based on this, the idea is to control inputs by directly mapping the estimation of the muscle activations, e.g. via ElectroMyoGraphic(EMG) sensors, on the exoskeleton. The control policy resulting from this mapping acts in feedforward in a way to exploit the muscle-like dynamics of the mechanical device. Thanks to the particular structure of the actuator, the exoskeleton joint stiffness naturally results from that mapping. The platform as well as the novel control idea have been experimentally validated and the results show a substantial reduction of the subject muscle effort.

Fig. 1. FLExo , a 1DoF upper limb exoskeleton based on human muscle dynamics analogy.

I. Introduction

Recent developments in assistive and rehabilitation robotics move towards the design of soft machines to overcome the limitations that classical rigid robotic systems typically exhibit in dynamic and interactive tasks.

Extensive works have explored both the control and design of rigid robots for assistive applications. The reader is referred to [1] and [2] for a recent review on control methodologies for exoskeletons. Explored control techniques include position, torque, impedance, admittance and neuro-fuzzy controllers.

Kazerooni et al. [3] have designed a positive feedback based sensitivity amplification controller for Berkley Lower Extremity Exoskeleton (BLEEX) hydraulically actuated. The goal of the controller was to maximize the sensitivity to the forces and torques exerted by the pilot. A three Degree of Freedom (DoF) exoskeleton to assist forearm and wrist motion, named W-EXOS, has been proposed in [4] where a PD controller on the DC motors position was applied to track the desired motion. In [5] an EMG based torque control approach for an exoskeletal knee is presented.

Recently a novel emerging trend that exploits compliant actuators in such assistive applications emerged. The compliance has been introduced in the robotic actuation with fixed or variable stiffness elements (see [6] for an extensive review) to shape and enrich the robot dynamic behavior [7] [8]. In [9] it has been recognized that (i) assistive robots should be compliant and avoid to interfere with the natural motion of the human joints, and (ii) artificial muscles should behave rigidly to support larger forces when helping in strenuous motor tasks. In [10] and [11] exoskeletons with fixed physical compliance embedding rotary series elastic acturators(SEA) have been presented and controlled in torque mode. The SEAs decouple the motor inertia from the human thanks to the spring, reducing undesired interaction forces - a prerequisite in order to make the human master in human-robot interaction [11]. Other recent works, as [12], developed an upper limb exoskeleton, the NeuroExo, powered by an antagonistic variable stiffness actuator(VSA) controlled in position and stiffness mode without applying human intention(e.g. through EMG) in feedback. Integrating a passive VSA in the exoskeleton gives the benefit of guaranteeing low output impedance even in case of high frequency disturbances [13]. The same doesn't hold for a system with rigid actuators controlled in closed loop. Vitiello et al. [13] also present the NeuroExos controlled in passive-compliance and torque mode. Lefeber et al. in [14] use a position controlled Maccepa, the mechanically adjustable compliance and controllable equilibrium position actuator, in an exoskeleton-type rehabilitation robot ALTACRO. It is interesting to point out that the adoption of variable stiffness introduces a new variable in the equation. This is why, more recent studies started to tackle the problem of deciding a policy for stiffness control. As an example [15] proposes to copy the user stiffness in the assistive device with very

This work was supported by the European Commission projects (Horizon 2020 research program) SOFTPRO (no. 688857)

[1]Research Center "Enrico Piaggio", University of Pisa, Largo Lucio Lazzarino 1, 56126 Pisa, Italy

[2]Department of Advanced Robotics, Istituto Italiano di Tecnologia, via Morego, 30, 16163 Genova, Italy

sariah25_mghames@hotmail.com

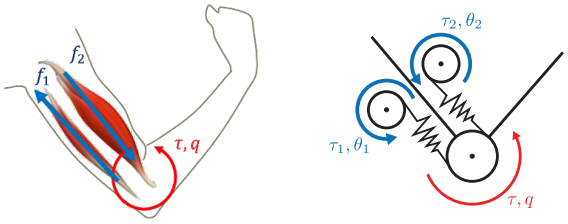

(a) (b)

Fig. 2. Human (a) and robotic (b) agonist-antagonist actuation systems with main variables underlined. q is in both cases the joint angle, and τ is the external torque. f_1 and f_2 are the forces exerted by the biceps and triceps respectively. θ_1 and θ_2 are the motor angles, while τ_1 and τ_2 are the respective exerted torques.

promising outcomes for the selected task.

In all the aforementioned approaches the exoskeletons are controlled so as to present a desired behavior, through a feedback control loop. However, it was shown in [16] that the use of feedback action in soft robots corresponds to a change in the natural behavior of the system, altering or altogether erasing the mechanical intelligence purposefully introduced in the design.

In this paper we introduce the idea of controlling an antagonistic VSA mechanism by exploiting the analogy that exists between its inputs and the ones of a human pair of muscles. We show that by a proper selection of VSA spring characteristics both systems can behave similarly. The proposed control policy maps in feedforward the estimated muscle activation directly on the robotic counterpart, thus preserving the natural dynamic of the system.

According to these considerations we also present the design of both the mechanics and control of FLExo ; a new soft assistive exoskeleton device following the dynamics of human muscles. The device and the control are experimentally validated in performing both stationary and dynamic tasks, recording user effort. In particular two different control strategies are tested and compared, showing a substantial reduction of the user effort.

II. Human Muscle Augmentation

A. Agonist-antagonist muscle model

According to [17], it is possible to describe the force exerted by a muscle on the corresponding joint as exponential function of the muscle activation A. The activation is proportional to the difference between the current muscle length l and the threshold length $\lambda(t)$ which assumes here the role of an input. Moreover, a term proportional to the variation of muscle length $\dot{l}$ is considered. The overall activation can thus be written as

$$A(t) = [l(t-d) - \lambda(t) + \mu(t)\dot{l}(t-d)]^+, \tag{1}$$

where $[x]^+$ is 0 when $x \leq 0$, and x otherwise. The reflex delay d can be observed during the unloading response of human arm muscles.

Since any muscle has at least an antagonistic one acting on the same joint, we consider here the most simple actuation element of the human neuro-muscle-skeletal system, an antagonistic pair of muscles. According to [17] the forces f_1 and f_2 exerted by the two muscles are

$$\begin{aligned} f_1 = &\ \rho(e^{\delta A_1} - 1), \quad f_2 = -\rho(e^{\delta A_2} - 1) \\ A_1 = &\ Rq(t-d) - \lambda_1(t) + \mu(t)R\dot{q}(t-d) \\ A_2 = &-Rq(t-d) + \lambda_2(t) - \mu(t)R\dot{q}(t-d), \end{aligned} \tag{2}$$

referring to the previous equation q is the forearm angular position w.r.t. the arm, and R is the instantaneous lever arm, i.e. $l = Rq$.

The force balance of an agonist-antagonist muscle pair acting on a same joint is (see Fig. 2(a))

$$\tau + R(f_1 + f_2) = 0, \tag{3}$$

where τ is the external torque. By considering the force equilibrium in static condition in presence of no external load (i.e. $\tau = 0$, $\dot{q} = 0$), from Eqs. (2) and (3) it results

$$\begin{aligned} & f_1 = -f_2 \\ \Rightarrow \quad & e^{\delta(Rq-\lambda_1)} = e^{\delta(-Rq+\lambda_2)} \\ \Rightarrow \quad & q = \frac{r}{R}. \end{aligned} \tag{4}$$

where $r := \frac{\lambda_1+\lambda_2}{2}$ is referred in literature as r-command. The stiffness at the equilibrium σ is defined as the derivative of the external torque τ w.r.t. the link position

$$\sigma = \left.\frac{\partial \tau}{\partial q}\right|_{q=\frac{\lambda_1+\lambda_2}{2R}} = 2\rho\delta R^2 e^{\delta c} \tag{5}$$

where $c := \frac{\lambda_2-\lambda_1}{2}$, which is referred in literature as c-command or co-activation.

B. A robotic counterpart

Leveraging on the human example, many actuator designs were proposed in robotic literature in which a compliant behavior is purposefully introduced in the design. In Variable Stiffness Actuators (VSA) such characteristics can be adjusted online in analogy to the human ability to modulate joint stiffness. For an extensive review please refer to [6].

For the purposes of the present work, the robotic counterpart of specific interest is the VSA antagonistic architecture (see e.g. [18]). Fig. 2(b) shows the mechanism sketch. Two motors are connected to the output shaft through a set of non-linear springs. Each motor together with the corresponding set of springs, represents a muscle. In [19] the choice of the non-linear characteristic of the spring was discussed, comparing it to the overall mechanical characteristic of a muscle pair.

In analogy to (2) the following characteristics is proposed

$$\tau_1 = \gamma e^{\beta(q-\theta_1)} - \mu, \quad \tau_2 = -\gamma e^{\beta(-q+\theta_2)} + \mu. \tag{6}$$

where τ_1 and τ_2 are the torques that each motor applies to the link, and β, γ, μ are constants depending on the choice of mechanical elements. Figure 3(b) shows three different results obtained for the VSA torque-deflection characteristics. Setting all parameters presented in 6 there, approximations of the experimental curves are

TABLE I

EQUIVALENCES IN HUMAN AND ROBOTIC ACTUATION

	Muscle	VSA
Equilibrium Position	$\frac{\lambda_2+\lambda_1}{2R}$	$\frac{\theta_2+\theta_1}{2}$
Stiffness	$2\rho\delta R^2 e^{\delta\frac{\lambda_2-\lambda_1}{2}}$	$2\gamma\beta e^{\beta\frac{\theta_2-\theta_1}{2}}$
Inputs	$\frac{\lambda_1}{R}$, $\frac{\lambda_2}{R}$	θ_1, θ_2
Co-Activation amplification	δ	βR
Minimum stiffness	$\rho\delta$	$\gamma\beta$

reported. Putting together torque-deflection characteristics in biological and robotic systems, figures 3(a) and 3(b) show the existing similarities.

As in (3) we impose the equilibrium of forces

$$\tau+\tau_1+\tau_2=0\,, \tag{7}$$

where τ takes into account the external load, and τ_1, τ_2 are the torques applied by the motors to the link. By considering the force equilibrium in static condition in presence of no external load (i.e. $\tau=0$, $\dot{q}=0$), from Eqs. (6) and (7) yields

$$\begin{aligned} & \tau_1=-\tau_2 \\ \Rightarrow\quad & e^{\beta(q-\theta_1)}=e^{\beta(-q+\theta_2)} \\ \Rightarrow\quad & q=\frac{\theta_1+\theta_2}{2}. \end{aligned} \tag{8}$$

The stiffness σ can be obtained as a function of θ_1 and θ_2 by determining the derivative of the external torque w.r.t. the link position q evaluated in the equilibrium, i.e.

$$\sigma=\left.\frac{\partial\tau}{\partial q}\right|_{q=\frac{\theta_1+\theta_2}{2}}=2\gamma\beta e^{\beta\frac{\theta_2-\theta_1}{2}}\,. \tag{9}$$

Thus, by looking at Eqs. (2), (4), (5) for human actuation and Eqs. (6), (8), (9) for robotic actuation, it clearly results that motor positions θ_1, θ_2 have the same role of activation lengths λ_1, λ_2. Furthermore, by proper choice of system parameters the two behaviors are equivalent, as summarized in Table I.

In the opinion of the authors the presented similarities between VSA and muscular systems could be profitably employed with the long term goal of designing assistive robots powered by artificial muscles to act in parallel with the human joints.

In the following section two simple control laws taking advantage of the similarities between the artificial and natural joint, are proposed and experimentally validated.

III. CONTROL POLICY

Several policies can be used to map the human intention into the robotic actuator. Taking advantage of the equivalence discussed in the previous section, we propose here to control the actuator directly by mapping λ on their robotic counterpart, thus looking at the VSA as a pair of artificial muscles augmenting directly the natural pair.

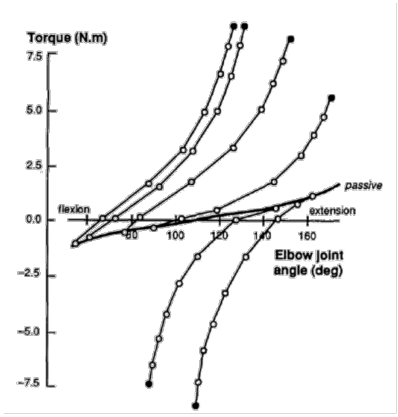

(a)

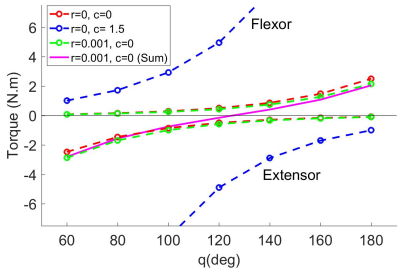

(b)

Fig. 3. Torque-Deflection characteristics in robotic and biological system. In (a) is presented the elastic characteristic of agonist and antagonist muscles acting on human elbow joint, taken from [17]. In (b) is presented the antagonistic arrangement VSA characteristics for different values of equilibrium point r and stiffness c and for the same joint angle range as the one shown in (a). Each characteristic reported results from the fitting of τ_1 and τ_2 given by Eq. 6.

By considering the human joint at a static equilibrium (i.e. $\dot{q}=0$) it is possible to solve Eq. (2) for λ_1 and λ_2 as

$$\begin{cases} A_1=+Rq-\lambda_1 \\ A_2=-Rq+\lambda_2 \end{cases} \quad\Longrightarrow\quad \begin{cases} \lambda_1=-A_1+Rq \\ \lambda_2=+A_2+Rq\,. \end{cases} \tag{10}$$

Since $\theta_1=\frac{\lambda_1}{R}$, $\theta_2=\frac{\lambda_2}{R}$ (see table I), the mapping between muscles and their robotic counterparts can be implemented as

$$\begin{cases} \theta_1=q-\frac{A_1}{R} \\ \theta_2=q+\frac{A_2}{R}. \end{cases} \tag{11}$$

Surface EMG sensors are classically used in literature as a useful measure of muscular activation [20]. A vast literature on the estimation of neural strategies from EMG exists, see e.g. [21] [22]. By reference to [23], "EMG electrodes are used to detect a motor unit action potential(MUAP) which is modeled as the combination of muscle fiber action potentials from all muscle fibers of a single motor unit". Since we are considering a limited surface area of the muscle, we approximate here the muscle fiber activation A_i as proportional to the envelope of the correspondent EMG signal E_i, deputing to future work the implementation of more sophisticated algorithms. Thus the overall mapping

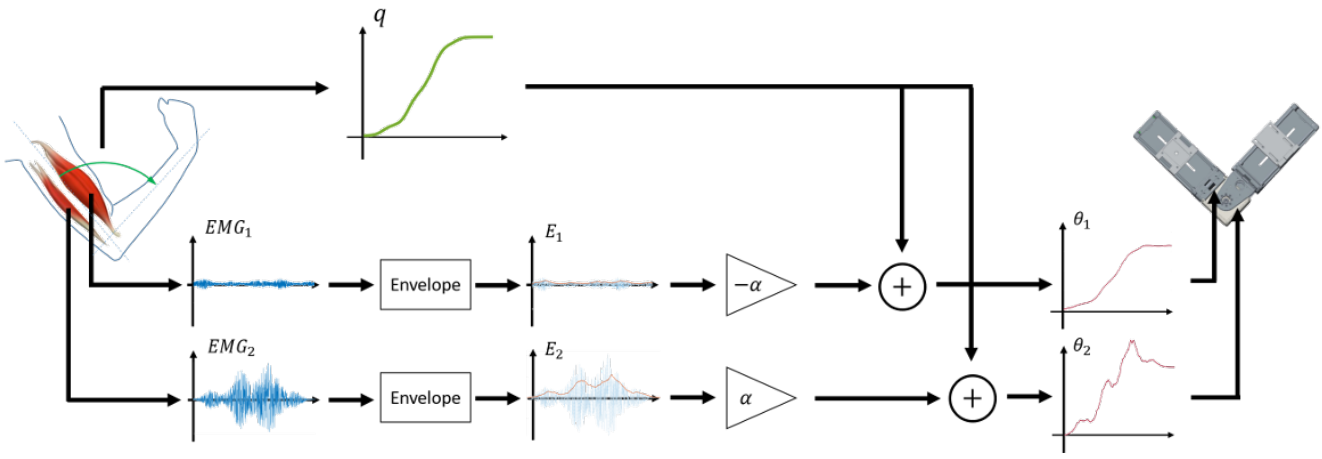

Fig. 4. Sketch of the scheme considered in this work. Thanks to the described equivalence between a pair of human muscles and the proposed exoskeleton, we can control it by mapping the estimation of the muscle activation lengths λ directly on their robotic counterparts θ.

results (see Fig.4)

$$\begin{cases} \theta_1 = q - \alpha E_1 \\ \theta_2 = q + \alpha E_2 \end{cases} \tag{12}$$

where α is considered as a gain. Note that in Eq. (12) the estimated desired muscle length of the subject is directly mapped on its robotic counterpart, without the need of any additional control loop. In this way the muscle-like dynamics of the actuator is exploited, instead of being canceled [16].

As it will result evident from the experimental validation of Sec. V, a control rule as in Eq. (12) succeeds in augmenting the user performance. In order to test the possibility of a complete transition of the effort from the user to the exoskeleton, in the following we will test the use of a feedback action proportional to the integral of the measured activation

$$\begin{cases} \theta_1 = q - (\alpha E_1 + \beta \int_0^t E_1 - E_2 \, \mathrm{d}\tau) \\ \theta_2 = q + (\alpha E_2 + \beta \int_0^t E_2 - E_1 \, \mathrm{d}\tau) \end{cases} \tag{13}$$

We removed the effect of co-activation from the integral feedback to avoid divergence that could be generated by the integration of a constant value. Such integral action should take care of errors due to model mismatching, and convey a full shift of the effort from the human arm to the exoskeleton. The parameters α and β are considered here as two control gains, that we tune heuristically. We demand to future work the automatic choice of α and β based e.g. on formal model identification. For safety concerns, the control inputs are saturated.

IV. Design

In this section we consider the design of FLExo , a 1DoF upper limb exoskeleton actuated through a VSA reproducing the antagonist muscle pair behavior.

A. Mechanical Requirements

For the elbow exoskeleton, the most demanding task in terms of torque is when the forearm, together with a payload, passes through a position normal to the upper arm. The average male forearm weight is 1.36Kg and the hand 0.46Kg. The average male distance of the center of gravity from the elbow joint is 15.49cm for the forearm and 32.39cm for the hand [24]. Thus the resulting gravity torque at the elbow joint is 3.67Nm.

For dynamic movements, we consider here to work under 10 oscillation per minute, which is about $1\frac{\text{rad}}{\text{s}}$ (considering a joint extension of π).

Following these considerations we decided to use the *qbmove advance*, a derivation of the VSA cube [18] which is a variable stiffness actuator implementing the mechanical characteristic in Eq. (6) [19]. Like a pair of muscles acting on a natural joint, the *qbmove advance* mechanically implements the antagonistic principle via two motors connected to the output shaft through a non-linear elastic transmission implemented with linear springs. The *qbmove advance* can generate maximal constant torque equal to 6Nm, and has a maximum motor speed of $4\frac{\text{rad}}{\text{s}}$. The bandwidth frequency of the VSA actuator was experimentally determined to be 6Hz. Fore further details, the reader can refer to [18] , [25].

B. Mechanics

Fig. 5 presents the FLExo . The proposed soft wearable upper limb platform has 1 DoF, actuated through qbmove, the actuator discussed in the previous section. Such actuator was designed as part of the open-source platform Natural Machine Motion Initiative (NMMI) [25], and thus share with it a standardized hardware interface.

We designed the exoskeleton support in order to have the actuator output axis coincident as close as possible with the user elbow axis. In future versions, we will adopt different designs of the mechanism that can relief the alignment problem (e.g [12]). Each side of the actuator is connected to the user limb through four modular elements, (1), (3), (4), (5)

in Fig. 5. The mechanical flanges (1) are standard elements provided by NMMI platform, used as mechanical interface for the customized parts. The plastic link (3) is connected to (1) and in the final configuration it is parallel to human arm. Elements (4) and (5) are connected orthogonally to (3), and are designed to interface the exoskeleton with the user's limb.

As shown in Fig. 6, elements (3),(4),(5) are designed such that they can be mounted at different distances, in order to fit the exoskeleton to different limb sizes. Elements (4) and (5) are inserted in the sliding bars of each parallel link respectively. The translation along the bars is fixed by creating a horizontal groove along the parallel link (3) and a hole in the the normal link (4).

Since the target of FLExo is to serve as testbed for natural upper limb assistance, user comfort is an important issue that was considered in the design. To avoid injuries or painful tightening during dynamic motion, soft tissues are applied to the normal plastic links through off-the-shelf motorcycle arm cover modules (6). The two modules, one for the forearm and the other for the upper arm, are screwed to the links (5).

Due to the assistive nature of the system we included in the FLExo a gravity compensation mechanism. An off-the-shelf gravity compensation arm [26] is connected to the rest of the structure through a custom bearing shaft (8) pointing out of the actuator into the cubic element (7), as in Fig. 5. The bearing allows free motion of the whole exoskeleton-arm system in the sagital/transverse plane. The amount of compensation can be manually regulated, in order to obtain a full compensation of the whole limb or just of the exoskeleton weight.

An important feature of the gravity compensation platform is the motion modularity it can provide: By rotating the shaft linking the cubic element (7) to the gravity compensation arm by 90°, we can change the motion from the sagital plane to the transverse plane (as in Fig. 7).

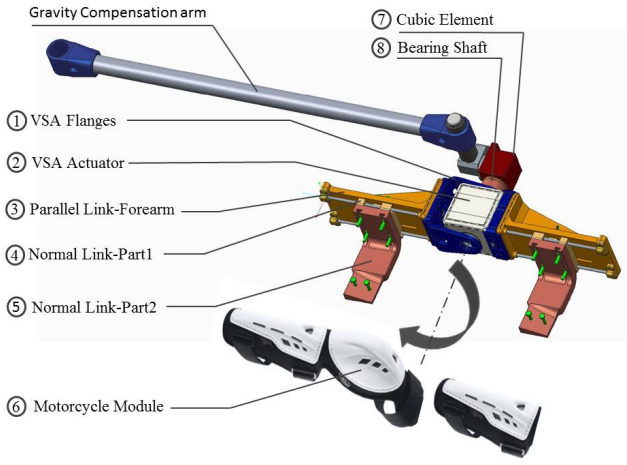

Fig. 5. FLExo CAD with main components depicted.

Note that the elbow joint range for a human aged 22-44 is [-94.7°, 60°] (straighten out forearm, bringing forearm to the biceps) where the 0° corresponds to the normal position between forearm and upper arm [27]. The range of motion of the exoskeleton output shaft is [-180°,180°], and thus completely contains the range of motion of the human joints of interest. For safety issues, mechanical stops are mounted to the device to avoid exceeding the user joint range of motion.

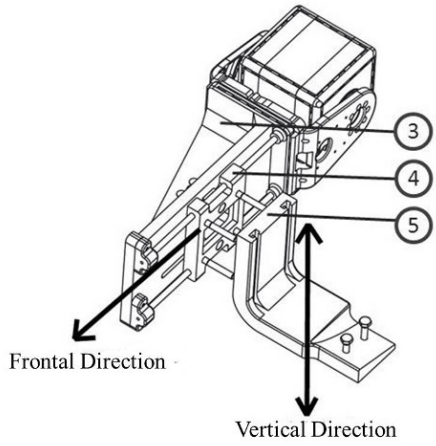

Fig. 6. The joint misalignment mechanism allows the configuration of FLExo for limbs of different sizes.

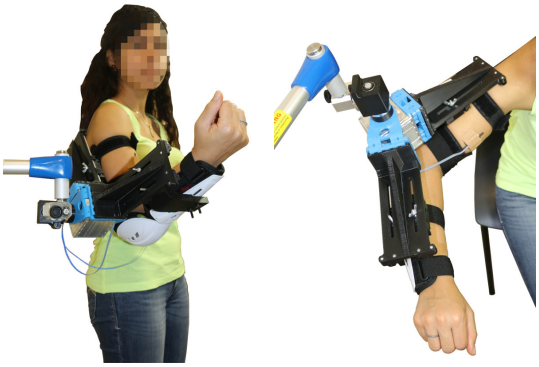

(a) (b)

Fig. 7. FLExo available configurations: (a) vertical and (b) horizontal

C. Electronics

To control the FLExo user intention is estimated (desired elbow angular position and stiffness) by acquiring EMG signals on the surface of the upper arm muscles. Two Ottobock surface EMG sensors, held together by an elastic band, are used to measure the EMG signals (figure 8). One EMG is placed on the bicep brachii along the line *medial acromion - fossa cubit* at $1/3$ from the fossa cubit while the other sensor is placed on the tricep bracchi at $1/3$ the line *posterior crista of acromion - olecranon*[28].

The Ottobock sensors are connected to a custom board [29]. The signals provided by the Ottobock sensors are rectified and filtered. The actuator is powered by a 24V 6 cells lithium battery. All the electronics used is part of NMMI platform, and its design is available on the initiative website

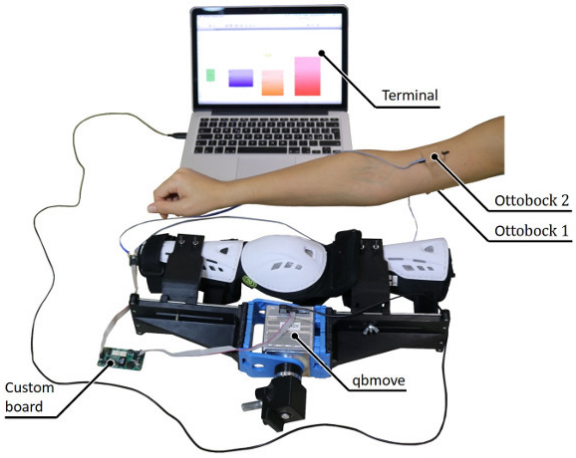

Fig. 8. FLExo electronics. Two surface Ottobock EMG sensors are used to acquire muscle activations. A custom board interfaces with Ottobock electronics. Such board is connected in daisy chain with qbmove electronics, to the terminal where the controller is implemented.

[25]. Qbmove actuator and Ottobock sensors acquisition board are connected in daisy chain to a terminal running Matlab/Simulink (MATLAB 9.1, The MathWorks Inc., Natick, MA, 2016), where the exoskeleton control policy can be implemented.

V. Experimental Validation

A. Experimental Setup

The validation of the FLExo has been made through the implementation of the control strategies of Eq. (12) and (13). The muscle's envelopes E_1 and E_2 are extracted from EMG signals. Ottobock's sensors output directly EMG envelope that is already high pass filtered and rectified. Furthermore an additional filter action is applied through a second-order 10 Hz low-pass filter. The data acquisition was performed at a sufficiently high rate of 200 Hz compared to the highest frequency adopted during the conducted experiments, 0.2Hz. Since the EMG characteristic of a muscle is strongly position and subject dependent [30], a calibration procedure is needed before the experimental session. This procedure starts with the subject standing and the arm lying along the torso, with the elbow to its full extended position ($q \simeq -90°$). At first the subject completely relaxes the arm. In this phase the EMG signals are acquired for 3 seconds and their maximum value is taken as the bias B_1 and B_2 of the respective signals. Then, the calibration continues asking the subject to stiffen the elbow as high as possible for 3 seconds. The mean values of the acquired signals are taken as maximum voluntary contraction [31], [32] relative to that specific elbow angular position q. This second step is repeated for 3 equidistant angular positions, spanning the whole range of the exoskeleton. The acquired points from these acquisitions are first biased by B_1 and B_2, as previously calculated, and then fitted with two second order polynomials P_1 and P_2. During the experiments, the filtered sensor signals are normalized by these polynomial, giving the envelopes as

$$E_i(t) = \frac{EMG_i(t) - B_i(t)}{P_i(q)}, \tag{14}$$

where EMG_i is the output signal of each sensor.

The measurements are related to the force exerted by the muscles. Therefore, the integral of the envelopes over the experiment duration is used to evaluate the performance of the different controls. This index is called *Energy Consumption Index* (*ECI*) and defined as

$$ECI = \int_{T_0}^{T_f} (E_1(t) + E_2(t))dt\,, \tag{15}$$

where T_0 and T_f are the initial and final instant of the experiment. This is a common index to evaluate the performances of assistive exoskeletons, similar e.g. to the ones proposed in [33].

The experiments can be divided in two sets. The first set evaluates the control strategy in a static scenario: the subject has to maintain the upper arm along the torso and hold the forearm parallel to the floor, i.e. $q = 0°$. In the plots of Fig. 9 the results of control of Eq. (12), tested with different values of α are reported. The same comparison for Eq. (13) is shown in Fig. 10, with $\alpha = 400°$ and $\beta = 0, 5, 8, 20[deg/s]$. Additionally, Fig. 11 shows the results of the same task for both controls when an external load of 0.5 Kg is applied on the subject forearm. In all these three cases E_1 was always null, since in the static position only the biceps is involved in the holding effort.

The second type of experiments aims at investigating the performance of the described controls on a dynamic task. The subject was asked to perform a periodical motion, moving the forearm from totally flexed to totally extended, following an audio signal at 10 pulse per minute.

The results are depicted in Fig. 12, where the two controllers are compared and the evolution of E_1 is also reported.

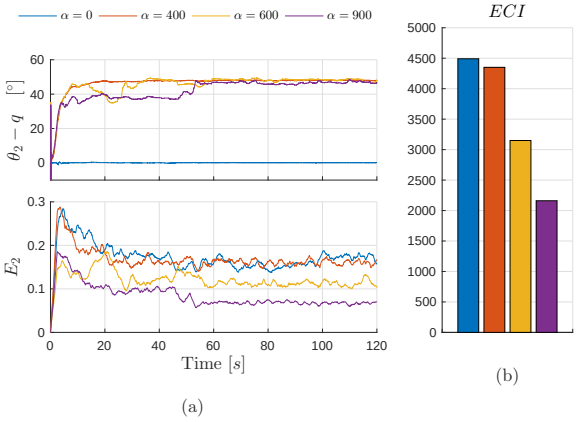

Fig. 9. Static experiment: hold the position $q = 0°$ with the control low of Eq. (12). (a) Evolution in time, (b) Energy Consumption Index

B. Discussion

Analyzing the results of the static experiment of Fig. 9.a it is possible to see the envelope E_2 decreasing proportionally

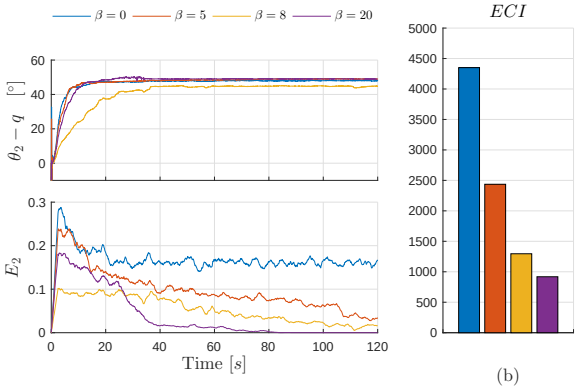

(a) (b)

Fig. 10. Static experiment: hold the position $q = 0°$ with the control low of Eq. (13) and $\alpha = 400°$. (a) Evolution in time, (b) Energy Consumption Index

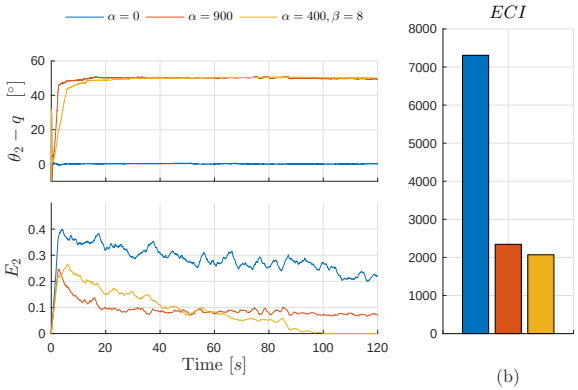

(a) (b)

Fig. 11. Static experiment: hold the position $q = 0°$ with an external load of $0.5\,Kg$. (a) Evolution in time, (b) Energy Consumption Index

to the set value of α. A confirmation of the performance is given in Fig. 9.b, where the lowest value is recorded for the highest gain, i.e. $\alpha = 900°$.

The same trend can be appreciated also with the introduction of the integral contribution (Fig 10). *ECI* decreases with the increment of the gain β. Furthermore, it is possible to see that a higher integral gain increments the velocity reduction of the muscle envelope (i.e. in Fig- 10.a E_2 reaches the zero in the time window of 120 seconds only when $\beta = 20°/s$). The different performance of the two control strategies are highlighted in Fig. 11, where the external load is applied to the forearm. It is clear from the *ECI* (Fig. 11.b) that the integral action allows to substantially decrease the subject effort in the static case.

On the other hand, the plots shown in Fig. 12 suggest that in a dynamic situation the best performance is given when only the proportional control is active. Indeed, even if the average of E_2 slightly decreases when $\beta \neq 0$, the one of E_1 increases, due to the integral terms that act on the desired prime mover positions θ_1 and θ_2. Indeed, the spikes recorded for E_1 of plot Fig. 12.a occur when the arm movement is in the decreasing phase. In that phase the subject has to push against the exoskeleton, that is pulling up due to the integral term. As before, this analysis is confirmed by the *ECI* of Fig. 12.b: the lowest *ECI* is the one relative to the case with proportional control only.

The overall analysis suggests that an integral control is useful in static situation, while during dynamic tasks it could increase the subject effort and then deteriorate the exo assistance.

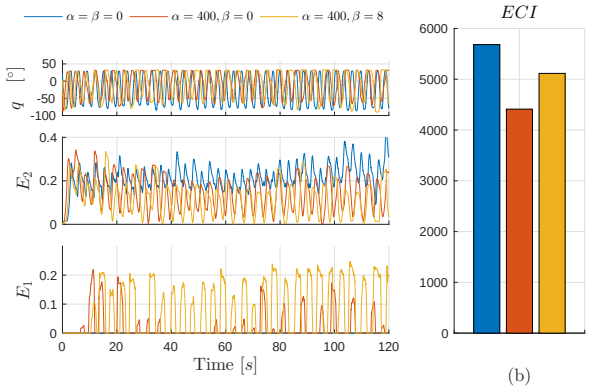

(a) (b)

Fig. 12. Dynamic experiment: sinusoidal trajectory at 10bpm. (a) Evolution in time, (b) Energy Consumption Index

VI. Conclusion

In this paper we have presented the FLExo , an assistive device whose dynamic reproduces the behavior of a pair of antagonistic muscles. The exoskeleton actuation system accepts inputs analoguous to the parameters controlled to generate an equilibrium position in antagonistic muscles (i.e. threshold lengths). The FLExo has been validated by implementing two different control laws that direclty map the estimated muscle activations to the respecive antagonistic motors. The FLExo joint stiffness results naturally from this mapping. First, a simple proportional controller driven by the user muscle activation, measured through surface electromyography, has been applied. Then, an integral action has been added to the controller. The two control policies have been tested both in static and dynamic tasks, showing a substantial reduction of user effort. In particular, results shown that a simple proportional controller is able to decrease muscle effort while holding a desired static or dynamic position while the additional integral term is able to minimize the effort to zero.

The control strategy design remains a very challenging task, a complete analysis of the control problem for such a system is beyond the scope of this paper and it is postponed as future work. Additional work will be devoted to study more in depth the problems of estimating muscle threshold lengths and testing different policies to map them to the FLExo .

Acknowledgment

The authors want to thank Giacomo Dinuzzi and Fabio Bonomo for their valuable support in the development of

the hardware prototype.

REFERENCES

[1] T. Proietti, V. Crocher, A. Roby-Brami, and N. Jarrass, "Upper-limb robotic exoskeletons for neurorehabilitation: A review on control strategies," *IEEE Reviews in Biomedical Engineering*, vol. 9, pp. 4–14, 2016.

[2] J. Gunasekara, R. A. Gopura, T. Jayawardane, and S. Lalitharathne, "Control methodologies for upper limb exoskeleton robots," in *IEEE-SICE International Symposium on System Integration (SII 2012)*, pp. 19–24, IEEE-SICE, 2012.

[3] H. Kazerooni, J.-L. Racine, L. Huang, and R. Steger, "On the control of the berkeley lower extremity exoskeleton (bleex)," in *IEEE International Conference on Robotics and Automation(ICRA 2005)*, pp. 4364–4371, IEEE, 2005.

[4] R. A. Gopura, *Development and Control of Upper-Limb Exoskeleton Robots*. PhD thesis, Univ. of Saga, Japan, 2009.

[5] C. Fleischer and G. Hommel, "Torque control of an exoskeletal knee with emg signals," *Berichte 1956*, vol. 79, 2006.

[6] B. Vanderborght, A. Albu-Schäffer, A. Bicchi, E. Burdet, D. G. Caldwell, R. Carloni, M. Catalano, O. Eiberger, W. Friedl, G. Ganesh, *et al.*, "Variable impedance actuators: A review," *Robotics and autonomous systems*, vol. 61, no. 12, pp. 1601–1614, 2013.

[7] D. Rus and M. T. Tolley, "Design, fabrication and control of soft robots," *Nature*, vol. 521, no. 7553, pp. 467–475, 2015.

[8] A. Albu-Schaffer, O. Eiberger, M. Grebenstein, S. Haddadin, C. Ott, T. Wimbock, S. Wolf, and G. Hirzinger, "Soft robotics," *IEEE Robotics & Automation Magazine*, vol. 15, no. 3, pp. 20–30, 2008.

[9] C. Majidi, "Soft robotics: A perspectivecurrent trends and prospects for the future," *Soft Robotics (SoRo)*, vol. 1, no. 1, p. e0148942, 2013.

[10] K. Kong and M. Tomizuka, "Control of exoskeletons inspired by fictitious gain in human model," *IEEE-ASME Transactions on Mechatronics*, vol. 14, no. 6, pp. 689–698, 2009.

[11] H. Vallery, *Stable and User-Controlled Assistance of Human Motor Function*. PhD thesis, Technical Univ. of Munich, Munich, December 2008.

[12] T. Lenzi, N. Vitiello, S. M. De Rossi, S. Roccella, F. Vecchi, and M. C. Carrozza, "Neuroexos: a variable impedance powered elbow exoskeleton," in *IEEE International Conference on Robotics and Automation(ICRA 2011)*, pp. 1419–1426, IEEE, 2011.

[13] N. Vitiello, T. Lenzi, , S. Roccella, S. M. De Rossi, E. Cattin, F. Giovacchini, F. Vecchi, and M. C. Carrozza, "Neuroexos: a powered elbow exoskeleton for physical rehabilitation," *IEEE Transactions on Robotics*, vol. 29, no. 1, pp. 220–235, 2013.

[14] P. Cherelle, V. Grosu, P. Beyl, A. Mathys, R. Van Ham, M. Van Damme, B. Vanderborght, and D. Lefeber, "The maccepa actuation system as torque actuator in the gait rehabilitation robot altacroy," in *3rd IEEE International Conference on Biomedical Robotics and Biomechatronics*, pp. 27–32, IEEE, 2010.

[15] N. Karavas, A. Ajoudani, N. Tsagarakis, J. Saglia, A. Bicchi, and D. Caldwell, "Tele-impedance based stiffness and motion augmentation for a knee exoskeleton device," in *2013 IEEE International Conference on Robotics and Automation (ICRA)*, pp. 2194–2200, IEEE, 2013.

[16] C. Della Santina, M. Bianchi, G. Grioli, F. Angelini, M. Catalano, M. Garabini, and A. Bicchi, "Controlling soft robots: Balancing feedback and feeforward elements," *IEEE Robotics & Automation Magazine*, 2017.

[17] P. L. Gribble, D. J. Ostry, V. Sanguineti, and R. Laboissière, "Are complex control signals required for human arm movement?," *Journal of Neurophysiology*, vol. 79, no. 3, pp. 1409–1424, 1998.

[18] M. G. Catalano, G. Grioli, M. Garabini, F. Bonomo, M. Mancini, N. Tsagarakis, and A. Bicchi, "Vsa-cubebot: a modular variable stiffness platform for multiple degrees of freedom robots," in *IEEE International Conference on Robotics and Automation(ICRA 2011)*, pp. 5090–5095, IEEE, 2011.

[19] M. Garabini, C. Della Santina, M. Bianchi, M. Catalano, G. Grioli, and A. Bicchi, "Soft robots that mimic the neuromusculoskeletal system," in *Converging Clinical and Engineering Research on Neurorehabilitation II*, pp. 259–263, Springer, 2017.

[20] J. V. Basmajian, "Muscles alive. their functions revealed by electromyography.," *Academic Medicine*, vol. 37, no. 8, p. 802, 1962.

[21] D. Farina, R. Merletti, and R. M. Enoka, "The extraction of neural strategies from the surface emg," *Journal of Applied Physiology*, vol. 96, no. 4, pp. 1486–1495, 2004.

[22] M. Sartori, M. Reggiani, D. Farina, and D. G. Lloyd, "Emg-driven forward-dynamic estimation of muscle force and joint moment about multiple degrees of freedom in the human lower extremity," *PloS one*, vol. 7, no. 12, p. e52618, 2012.

[23] M. B. Reaz, M. Hussain, and F. Mohd-Yasin, "Techniques of emg signal analysis: detection, processing, classification and applications," *Biological procedures online*, vol. 8, no. 1, pp. 11–35, 2006.

[24] S. Plagenhoef, F. G. Evans, and T. Abdelnour, "Anatomical data for analyzing human motion," *Research quarterly for exercise and sport*, vol. 54, no. 2, pp. 169–178, 1983.

[25] C. Della Santina, C. Piazza, G. M. Gasparri, M. Bonilla, M. Catalano, M. Garabini, G. Grioli, and A. Bicchi, "The quest for natural machine motion," *IEEE Robotics & Automation Magazine*, vol. 1070, no. 9932/17, 2017.

[26] "Saebomas." `http://www.saebo.com/saebomas/`. website visited on November 2016.

[27] "Normal joint range of motion study." `http://www.cdc.gov/ncbddd/jointrom/`. website visited on November 2016.

[28] P. Zipp, "Recommendations for the standardization of lead positions in surface electromyography," *European Journal of Applied Physiology and Occupational Physiology*, vol. 50, pp. 41–54, 1982.

[29] "Emg adpater 1.schdoc." `http://www.naturalmachinemotioninitiative.com/`. website visited on November 2016.

[30] O. N. Barr AE, Goldsheyder D. and N. M., "Testing apparatus and experimental procedure for position specifc normalization of electromyographic measurements of distal upper extremity musculature," *Journal of Applied Biomechanics*, vol. 16, pp. 576–585, 2001.

[31] J. Yang and W. DA, "Electromyographic amplitude normalization methods: Improving their sensitivity as diagnostic tools in gait analysis," *Arch Phys Med Rehabil*, vol. 65, pp. 517–521, 1984.

[32] D. CJ, "The use of surface electromyography in biomechanics," *Journal of Applied Biomechanics*, vol. 13(2), pp. 135–163, 1997.

[33] E. Pirondini, M. Coscia, S. Marcheschi, G. Roas, F. Salsedo, A. Frisoli, M. Bergamasco, and S. Micera, "Evaluation of the effects of the arm light exoskeleton on movement execution and muscle activities: a pilot study on healthy subjects," *Journal of neuroengineering and rehabilitation*, vol. 13, no. 1, p. 1, 2016.